Available online at www.sciencedirect.com
ScienceDirect
Trans. Nonferrous Met. Soc. China 25(2015) 2624−2629
Transactions of Nonferrous Metals Society of China
www.tnmsc.cn

Effect of melt infiltration parameters on microstructure and mechanical properties of tungsten wire reinforced $(Cu_{50}Zr_{43}Al_7)_{99.5}Si_{0.5}$ metallic glass matrix composite

Ebrahim Karimi SAEIDABADI[1], Reza GHOLAMIPOUR[2], Behrouz GHASEMI[1]

1. Department of Materials and Metallurgical Engineering, University of Semnan, Semnan 35131-19111, Iran;
2. Iranian Research Organization for Science and Technology (IROST), Tehran 33531-36846, Iran

Received 9 September 2014; accepted 4 February 2015

Abstract: Using melt infiltration casting at different temperatures (965, 990 and 1015 °C) for different time (10 and 15 min), the composites of $(Cu_{50}Zr_{43}Al_7)_{99.5}Si_{0.5}$ bulk metallic glass reinforced with tungsten wires were produced. X-ray diffraction (XRD), scanning electron microscopy (SEM) and quasi-static compression tests were carried out to evaluate the microstructure and mechanical properties. The results show that the maximum ultimate compressive strength and strain-to-failure of about 1880 MPa and 16.7% were achieved, respectively, at the infiltration temperature of 965 °C for 15 min.
Key words: Cu-based bulk metallic glass matrix composite; melt infiltration; shear band; tungsten wire

1 Introduction

It did not last long from the discovery of the first bulk metallic glass (BMG) that, these novel engineering alloys proved their positions as potential materials in a wide range of technical applications based on a variety of unique physical, chemical and mechanical properties [1−5].

However, BMGs are known to possess extremely low ductility along with poor plastic deformation behavior at room temperature, which greatly confines their use in structural applications. To practically overcome this certain drawback, extensive works have been devoted to promote the mechanical properties of BMGs via different strategies [6−10].

Meanwhile, raising the ductility, i.e., the strain-to-failure of BMGs, in general, has been well accepted to be possible by developing in situ and ex situ BMG matrix composites (BMGMCs) [11−21].

In the case of ex situ BMGMCs, the crystalline fibers or second phase particles are placed in a mold as the reinforcement, and subsequently, BMG melt infiltrates into the preform [22−37]. Herein, there is a significant relationship between the major parameters of infiltration process, such as temperature and time, and the microstructure and mechanical properties of the finally produced BMGMC. In fact, these parameters are effective on diffusion and interfacial reactions between the BMG matrix and the reinforcement. Excessive diffusion and reaction will eventuate in the dissolution of the reinforcement and will ultimately cause the loss of mechanical properties [31,32,36,37]. Thus, it is very important to catch the optimal infiltration temperature and time to achieve the best possible mechanical properties [35,36,37].

Among various types of BMGs, Cu-based alloys have gained appreciable interest among researchers owing to advantageous properties, such as good engineering strength, low cost and high density [37]. QIU et al [27] have also suggested tungsten fibers for three reasons: high melting temperature, limited reaction with the matrix material and the increase of density of reinforced composite that can lead to a great increase of dynamic energy in dynamic deformation case.

In the present study, a $(Cu_{50}Zr_{43}Al_7)_{99.5}Si_{0.5}$ (mole fraction, %) BMG was chosen, which is of high strength and suitable glass forming ability (GFA) by nearly 10 mm of critical thickness [38] to produce a new Cu-based BMG/W wire composite using melt infiltration casting process. The microstructure and mechanical properties of the composite were discussed in detail.

Corresponding author: Reza GHOLAMIPOUR; Tel/Fax: +98-21-56276635; E-mail: rgholamipour@gmail.com
DOI: 10.1016/S1003-6326(15)63884-5

2 Experimental

Ingots of $(Cu_{50}Zr_{43}Al_7)_{99.5}Si_{0.5}$ (mole fraction, %) were prepared by arc melting of a mixture of high purity metal elements in Ti-gettered Ar atmosphere in a water-cooled copper crucible. The ingots were remelted several times to ensure homogenizing followed by suction casting into a water-cooled copper mold to make BMG rods with 3 mm in diameter.

Tungsten wires with 1 mm in diameter were straightened and cut into 50 mm in length and cleaned in an ultrasonic bath of acetone and ethanol. The wires were then placed in the sealed end of stainless steel tubes (304) with 4.3 mm in inner diameter. The volume fraction of W wires was up to 70%. The tubes were necked about 1 cm above the wires, and the BMG rods were then placed in the tubes above the neck. The assembly of the tubes was washed by repeated evacuation (up to 10^{-3} Pa) and purged with high purity Ar gas of 0.35 MPa for several times followed by heating at various temperatures (965, 990 and 1015 °C , all above the liquidus temperature of BMG [38]) and held for different time (10 and 15 min) in an electrical furnace. Finally, it was quenched in water.

Slices of composite specimens were cut by a low speed saw to prepare quasi-static compression test samples. The ends of the samples were lapped to ensure parallelism of each other. The mechanical properties were measured with a Santam testing machine. The gauge dimensions of specimens were 4.3 mm in diameter and 8.6 mm in length for compressive test and the strain rate was 10^{-4} s^{-1}. The phase characterization and microstructural observations were carried out by X-ray diffraction (XRD) with Cu K_α radiation and scanning electron microscopy (SEM).

3 Results and discussion

Figure 1 displays the X-ray diffraction patterns of the composites prepared at different infiltrating temperatures. In the patterns, the sharp diffraction peaks of W phase superimposed on the diffuse broad peaks of amorphous unreinforced matrix are visible, alongside with the occurrence of some smaller diffraction peaks. These small peaks do not correspond to the pattern of the pure reinforcement and imply that partial crystallization of the matrix in the form of new crystalline phases takes place during the infiltration process. This phenomenon also correlates well with the intensity reduction of the diffuse amorphous peaks in bulk metallic glass matrix composite patterns due to the increase of volume fraction of such crystalline phases. Phases like Cu_8Zr, $Cu_{10}Zr_7$ and Zr_2Cu in addition to W_2Zr and W_5Zr_3 (in the interfacial reaction layer) can be indexed as well in the diffraction patterns of the composites.

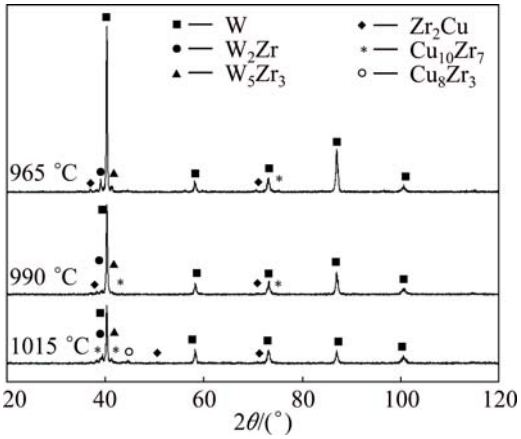

Fig. 1 XRD patterns of cross section of $(Cu_{50}Zr_{43}Al_7)_{99.5}Si_{0.5}$ BMG matrix composites prepared at different infiltrating temperatures (965, 990 and 1015 °C) for 15 min

The SEM images of the phases formed during the preparation of composites are shown in Fig. 2. They are identified as sphere-like, dendrite-like and polygonal phases. At low temperature of melt infiltration, a very narrow interfacial reaction layer can be observed, as shown in Fig. 2(a). The subsequent increase of temperature not only increases the reaction layer thickness, as shown in Fig. 2(d), but also increases the volume fraction of crystalline phases formed, by giving rise to thermally-activated reactions, i.e., the inter diffusion of matrix constituents and tungsten inside the matrix and near the interfacial regions. Moreover, the size and morphology of phases vary from sphere-like to dendrite-like and also polygonal morphology at elevated temperatures, which can be considered as another impact of such regional thermally-activated atomic interactions. The EDS analysis reveals that both sphere-like and polygonal phases marked with *A* in Figs. 2(a) and (c) are rich in Cu and Zr, as reported in Tables 1 and 2, and this is in consistency with the results obtained from the XRD patterns shown in Fig. 1.

It should be noted that the erosion of tungsten particles away from the wires and toward the matrix is an inevitable consequence of raising the process temperature and time, as shown in Fig. 2(c) by arrows.

Figure 3 shows the quasi-static compressive stress−strain curves of the composite samples. The total deformation and ultimate strength of the bulk metallic glass sample have been reported elsewhere [38], while for the composite sample prepared at 965 °C for 15 min, the ultimate compressive strength and strain at fracture are 1880 MPa and 16.7%, respectively. Any further increase of infiltration temperature or time makes the ultimate strength and total strain-to-failure of the

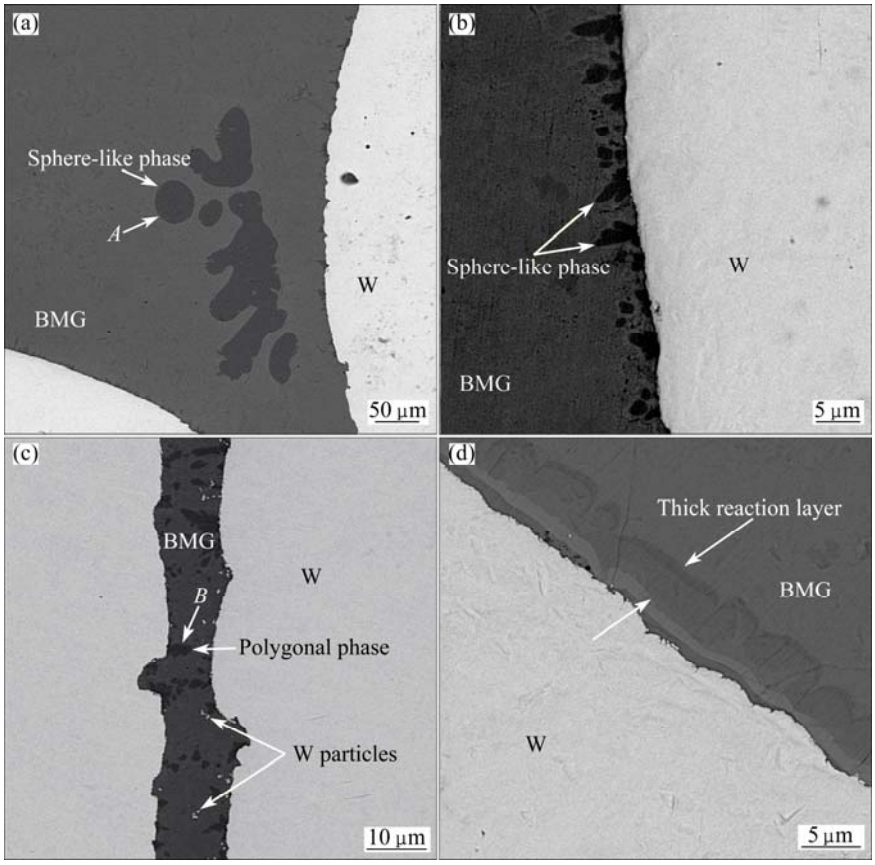

Fig. 2 SEM images of $(Cu_{50}Zr_{43}Al_7)_{99.5}Si_{0.5}$ BMG matrix composites prepared at different temperatures: (a) 965 °C for 15 min.; (b) 990 °C for 15 min.; (c) 1015 °C for 10 min; (d) 1015 °C for 15 min

Table 1 EDS analysis of components in sphere-like phase marked with *A* in Fig. 2(a)

Element	*w*/%	*x*/%
Al	9.9	22.6
Si	0.4	0.9
Cu	55.0	53.1
Zr	34.5	23.2
Total	100.0	100.0

Table 2 EDS analysis of components in polygonal phase marked with *B* in Fig. 2(c)

Element	*w*/%	*x*/%
Al	10.1	23.0
Si	0.4	0.9
Cu	53.4	51.7
Zr	35.9	24.2
Total	100.0	100.0

composites reduce. Figure 4 displays the specific absorbed energy or toughness (the area under the compressive stress−strain curves) of the composite samples that confirms the reduction in toughness by increasing the temperature or time of the infiltration process. It is also in good harmony with the results obtained from Fig. 2 in which the raised volume fraction of crystalline phases and the reaction layer formed at high temperatures might act as stress-concentration sites inside the matrix microstructure and thus deteriorate the mechanical properties of the composite.

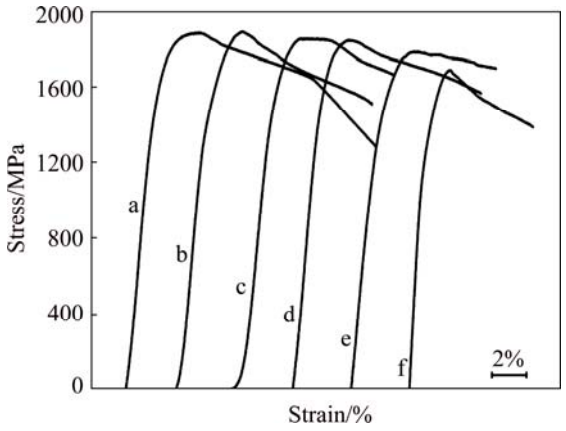

Fig. 3 Quasi-static compressive stress−strain curves of $(Cu_{50}Zr_{43}Al_7)_{99.5}Si_{0.5}$ BMG matrix composites prepared at different temperatures and time: (a) 965 °C for 15 min; (b) 965 °C for 10 min; (c) 990 °C for 10 min; (d) 990 °C for 15 min; (e) 1015 °C for 10 min: (f) 1015 °C for 15 min

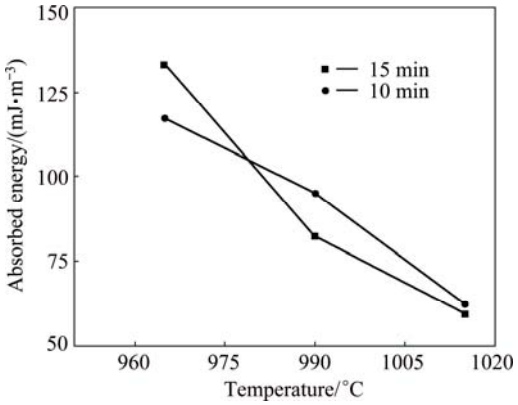

Fig. 4 Absorbed energy (toughness) versus temperature for composites prepared at temperatures of 965, 990 and 1015 °C for 10 and 15 min

Figure 5 shows the SEM micrographs of fracture features of the composites. Figure 5(a) shows the lateral view of W fibers (W_f)/BMGMC prepared at 965 °C for 15 min after compressive failure. A combination of primary shear bands (PSB), secondary shear bands (SSB), interactive shear bands (ISB), micro cracks (MC), and cracks [36], can also be observed in fracture surfaces of the same bulk metallic glass matrix composite, as shown in Figs. 5(b) and (c), which are significantly illustrative for the outstanding total fracture strain of the composite prepared at 965 °C for 15 min. The more the propagation of shear bands and cracks is blocked and/or deviated through certain mechanisms, the later the catastrophic failure of the composite takes place [16,37]. In Fig. 5(d), the track of one of these cracks is traced. Owing to the

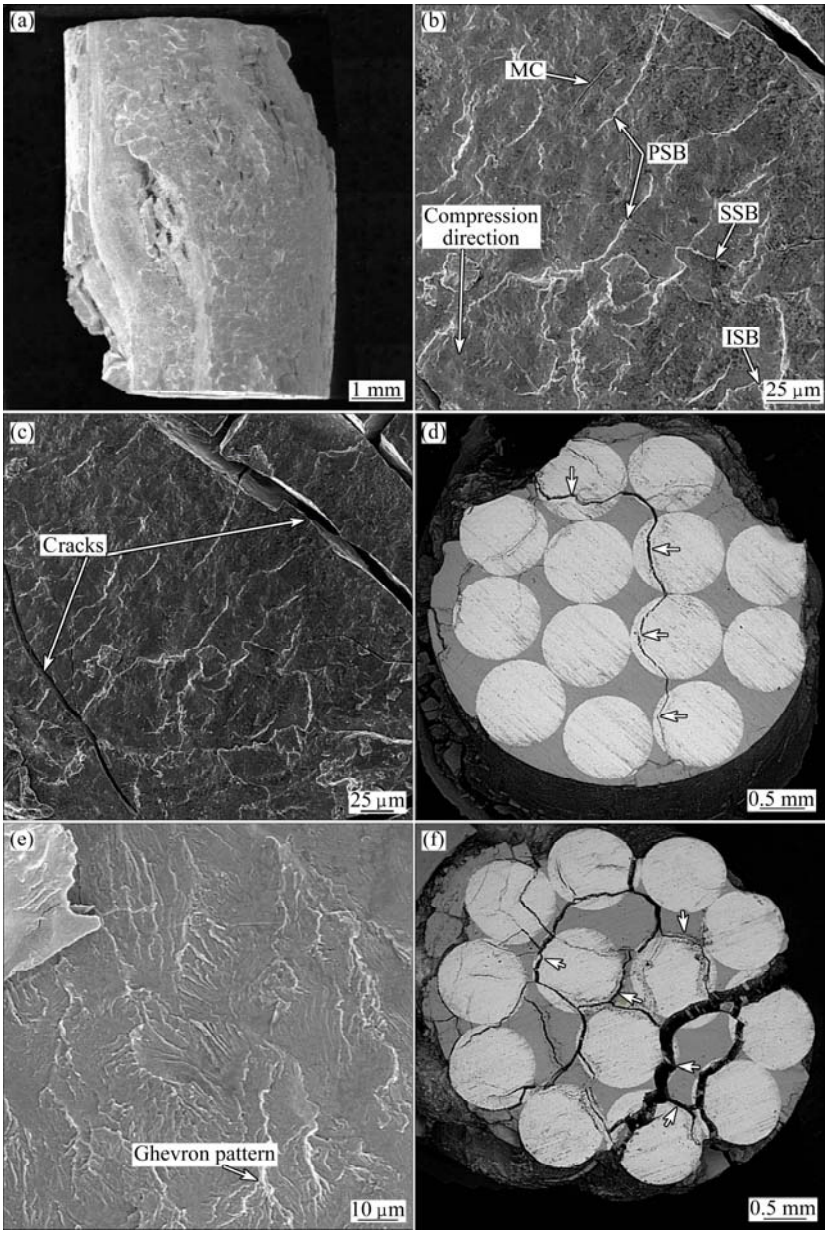

Fig. 5 SEM micrographs of fracture features of $(Cu_{50}Zr_{43}Al_7)_{99.5}Si_{0.5}$ BMG matrix composites prepared at 965 °C for 15 min (a−d) and 1050 °C for 10 min (e, f): (a) Lateral buckling; (b−d) Shear bands, micro cracks and cracks; (e, f) Shear bands , river-like mode of fracture and cracks

satisfactorily strong interfacial bonding between the matrix and W wires, the moving crack can not help passing through the wires with its tip becoming gradually blunt and its strain energy decreased, resulting in a higher toughness in BMGMC compared with the monolithic BMG. Besides the formation of visible chevron patterns as a result of the interaction, strike and branching of shear bands [33], the river-like mode of fracture in the sample prepared at 1015 °C for 10 min, as shown in Fig. 5(e), can be considered as another supporting idea for the enhanced toughness of the composite. While the weakening of the interface due to the formation of a thick reaction layer at 1015 °C, as shown in Fig. 5(f), changes the track of moving shear cracks from inside the wires to the weak interfacial regions, resulting in decreased strength and strain-to-failure of the composite compared with those prepared at low infiltrating temperatures [27,28]. When the stress approached the ultimate compressive strength (UCS), the failure is accompanied by buckling of reinforcing wires, as shown in Fig. 5(a).

4 Conclusions

1) The optimal conditions for melt infiltration process were proved to be 965 °C in temperature and 15 min in time through which the best mechanical properties, i.e., the ultimate strength of about 1880 MPa and total strain-to-failure of near 16.7% can be achieved under quasi-static compression test.

2) During the process, some crystalline phases formed and distributed in the matrix of the bulk metallic glass matrix composite, which have certain effects on the mechanical and fracture features especially at elevated infiltration temperatures and time.

References

[1] JOHNSON W L. Bulk amorphous metal—An emerging engineering material [J]. JOM, 2002, 54(3): 40−43.

[2] LOFFLER J F. Bulk metallic glasses [J]. Intermetallics, 2003, 11(6): 529−540.

[3] WANG W H, DONG C, SHEK C H. Bulk metallic glasses [J]. Materials Science and Engineering R, 2004, 44(2−3): 45−89.

[4] INOUE A, WANG X M, ZHANG W. Development and applications of bulk metallic glasses [J]. Reviews on Advanced Materials Science, 2008, 18: 1−9.

[5] INOUE A, TAKEUCHI A. Recent development and application products of bulk glassy alloys [J]. Acta Materialia, 2011, 59(6): 2243−2267.

[6] GUO S F, LI N, ZHANG C, LIU L. Enhancement of plasticity of Fe-based bulk metallic glass by Ni substitution for Fe [J]. Journal of Alloys and Compounds, 2010, 504(S1): s78−s81.

[7] PARK J M, WANG G, LI R, MATTERN N, ECKERT J, KIM D H. Enhancement of plastic deformability in Fe−Ni−Nb−B bulk glassy alloys by controlling the Ni-to-Fe concentration ratio [J]. Applied Physics Letters, 2010, 96(3): 031905.

[8] MAKINO A, Li X, YUBUTA K, CHANG C, KUBOTA T, INOUE A. The effect of Cu on the plasticity of Fe−Si−B−P-based bulk metallic glass [J]. Scripta Materialia, 2009, 60(5): 277−280.

[9] LEWANDOWSKI J J, GU X J, SHAMIMI NOURI A, POON S J, SHIFLET G J. Tough Fe-based bulk metallic glasses [J]. Applied Physics Letters, 2008, 92(9): 091918.

[10] LEWANDOWSKI J J, WANG W H, GREER A L. Intrinsic plasticity or brittleness of metallic glasses [J]. Philosophical Magazine Letters, 2005, 85(2): 77−87.

[11] CONNER R D, CHOI-YIM H, JOHNSON W L. Mechanical properties of $Zr_{57}Nb_5Al_{10}Cu_{15.4}Ni_{12.6}$ metallic glass matrix particulate composites [J]. Journal of Materials Research, 1999, 14(8): 3292−3297.

[12] KIM Y C, KIM D H, LEE J C. Formation of ductile Cu-based bulk metallic glass matrix composite by Ta addition [J]. Materials Transactions, 2003, 44(10): 2224−2227.

[13] QIN C L, ZHANG W, ASAMI K, KIMURA H, WANG X M, INOUE A. A novel Cu-based BMG composite with high corrosion resistance and excellent mechanical properties [J]. Acta Materialia, 2006, 54(14): 3713−3719.

[14] LI Y, POON S J, SHIFLET G J, XU J, KIM D H, LOFFLER J F. Formation of bulk metallic glasses and their composites [J]. MRS Bulletin, 2007, 32(8): 624−628.

[15] WANG H. Bulk metallic glass composites [J]. Journal of Materials Science and Technology, 2005, 21(S1): s86−s90.

[16] LIM H K, PARK E S, PARK J S, KIM W T, KIM D H. Fabrication and mechanical properties of WC particulate reinforced $Cu_{47}Ti_{33}Zr_{11}Ni_6Sn_2Si_1$ bulk metallic glass matrix composites [J]. Journal of Materials Science, 2005, 40(23): 6127−6130.

[17] LEE J C, KIM Y C, AHN J P, KIM H S. Enhanced plasticity in a bulk amorphous matrix composite: Macroscopic and microscopic viewpoint studies [J]. Acta Materialia, 2005, 53(1): 129−139.

[18] SIEGRIST M E, LOFFLER J F. Bulk metallic glass-graphite composites [J]. Scripta Materialia, 2007, 56(12): 1079−1082.

[19] PARK J S, LIM H K, PARK E S, SHIN H S, LEE W H, KIM W T, KIM D H. Fracture behavior of bulk metallic glass/metal laminate composites [J]. Materials Science and Engineering A, 2006, 417(1−2): 239−242.

[20] ZHU Z, ZHANG H, HU Z, ZHANG W, INOUE A. Ta-particulate reinforced Zr-based bulk metallic glass matrix composite with tensile plasticity [J]. Scripta Materialia, 2010, 62(5): 278−281.

[21] GUO S F, LIU L, LI N, LI Y. Fe-based bulk metallic glass matrix composite with large plasticity [J]. Scripta Materialia, 2010, 62(6): 329−332.

[22] QIU K Q, WU X F, WANG A M, ZHANG H F, DING B Z, HU Z Q. Salient shear bands and second-phase addition interactions of bulk metallic glass matrix composite [J]. Metallurgical and Materials Transactions A, 2003, 34(5): 1147−1152.

[23] DENG S T, DIAO H, CHEN Y L, YAN C, ZHANG H F, WANG A M, HU Z Q. Metallic glass fiber-reinforced Zr-based bulk metallic glass [J]. Scripta Materialia, 2011, 64(1): 85−88.

[24] CONNER R D, DANDLIKER R B, JOHNSON W L. Mechanical properties of tungsten and steel fiber reinforced $Zr_{41.25}Ti_{13.75}Cu_{12.5}Ni_{10}Be_{22.5}$ metallic glass matrix composites [J]. Acta Materialia, 1998, 46(17): 6089−6102.

[25] DANDLIKER R B, CONNER R D, JOHNSON W L. Melt infiltration casting of bulk metallic-glass matrix composites [J]. Journal of Materials Research, 1998, 13(10): 2896−2901.

[26] CHOI-YIM H, CONNER R D, SZUCES F, JOHNSON W L. Quasistatic and dynamic deformation of tungsten reinforced $Zr_{57}Nb_5Al_{10}Cu_{15.4}Ni_{12.6}$ bulk metallic glass matrix composites [J]. Scripta Materialia, 2001, 45(9): 1039−1045.

[27] QIU K Q, WANG A M, ZHANG H F, DING B Z, HU Z Q. Mechanical properties of tungsten fiber reinforced ZrAlNiCuSi

metallic glass matrix composite [J]. Intermetallics, 2002, 10(11−12): 1283−1288.

[28] WANG G, CHEN D M, SHEN J, STACHURSKI Z H, QIN Q H, SUN J F, ZHOU B D. Deformation behaviors of a tungsten-wire/bulk metallic glass matrix composite in a wide strain rate range [J]. Journal of Non-Crystalline Solids, 2006, 352(36−37): 3872−3878.

[29] QIU K Q, SUO Z Y, REN Y L, YU B. Observation of shear bands formation on tungsten fiber-reinforced Zr-based bulk metallic glass matrix composite [J]. Journal of Materials Research, 2007, 22: 551−554.

[30] CHOI-YIM H, LEE S Y, CONNER R D. Mechanical behavior of Mo and Ta wire reinforced bulk metallic glass composites [J]. Scripta Materialia, 2008, 58(9): 763−766.

[31] WANG M L, CHEN G L, HUI X, ZHANG Y, BAI Z Y. Optimized interface and mechanical properties of W fiber/Zr-based bulk metallic glass composites by minor Nb addition [J]. Intermetallics, 2007, 15(10): 1309−1315.

[32] QIU K Q, REN Y L. Melt infiltration casting of $Zr_{57}Al_{10}Nb_5Cu_{15.4}Ni_{12.6}$ amorphous matrix composite [J]. Journal of Minerals and Materials Characterization and Engineering, 2004, 3(2): 91−98.

[33] ZHANG H F, LI H, WANG A M, FU H M, DING B Z, HU Z Q. Synthesis and characteristics of 80 vol.% tungsten (W) fiber/Zr based metallic glass composite [J]. Intermetallics, 2009, 17(12): 1070−1077.

[34] ZHANG B Y, CHEN X H, WANG S S, LIN D Y, HUI X D. High strength tungsten wire reinforced Zr-based bulk metallic glass matrix composites prepared by continuous infiltration process [J]. Materials Letters, 2013, 93: 210−214.

[35] KHADEMIAN N, GHOLAMIPOUR R. Fabrication and mechanical properties of a tungsten wire reinforced Cu−Zr−Al bulk metallic glass composite [J]. Materials Science and Engineering A, 2010, 527(13): 3079−3084.

[36] KHADEMIAN N, GHOLAMIPOUR R. Study on microstructure and fracture behavior of tungsten wire reinforced Cu-based and Zr-based bulk metallic glass matrix composites [J]. Journal of Non-Crystalline Solids, 2013, 365: 75−84.

[37] KHADEMIAN N, GHOLAMIPOUR R. Effects of infiltration parameters on mechanical and microstructural properties of tungsten wire reinforced $Cu_{47}Ti_{33}Zr_{11}Ni_6Sn_2Si_1$ metallic glass matrix composites [J]. Transactions of Nonferrous Metals Society of China, 2013, 23(5): 1314−1321.

[38] MALEKAN M, SHABESTARI S G, ZHANG W, SEYEDEIN S H, GHOLAMIPOUR R, MAKINO A, INOUE A. Effect of Si addition on glass-forming ability and mechanical properties of Cu−Zr−Al bulk metallic glass [J]. Materials Science and Engineering A, 2010, 527(27): 7192−7196.

熔体渗透参数对钨丝增强$(Cu_{50}Zn_{43}Al_7)_{99.5}Si_{0.5}$非晶复合材料显微组织和力学性能的影响

Ebrahim Karimi SAEIDABADI[1], Reza GHOLAMIPOUR[2], Behrouz GHASEMI[1]

1. Department of Materials and Metallurgical Engineering, University of Semnan, Semnan, Iran;
2. Iranian Research Organization for Science and Technology (IROST), Tehran, Iran

摘　要：在不同的温度(965，990 和 1015 °C)和时间(10 和 15 min)下，使用熔体渗透铸造制备钨丝增强的$(Cu_{50}Zn_{43}Al_7)_{99.5}Si_{0.5}$块体非晶复合材料。通过 X 射线衍射、扫描电镜和准静态压缩实验表征材料的显微组织和力学性能。结果表明：在渗透温度为 965 °C 下保温 15 min 时制备的非晶复合材料，获得的最大极限抗压强度和失效应变分别为 1880 MPa 和 16.7%。

关键词：Cu-基块体非晶复合材料；熔体渗透；剪切带；钨丝

(Edited by Mu-lan QIN)